

## DNA at Aqueous/Solid Interfaces: Chirality-Based Detection via Second Harmonic Generation Activity

Faith C. Boman, Julianne M. Gibbs-Davis, Laurel M. Heckman, Brian R. Stepp, SonBinh T. Nguyen, and Franz M. Geiger\*

Department of Chemistry, Northwestern University, 2145 Sheridan Road, Evanston, Illinois 60208

Received October 10, 2008; E-mail: geigerf@chem.northwestern.edu

**Abstract:** We present electronic spectra of single-strand and duplex DNA oligonucleotides covalently attached to fused quartz/aqueous interfaces and demonstrate that a strong nonlinear optical linear dichroism response is obtained when adenine and thymine bases undergo Watson–Crick base pairing to form a double helix. Complementary  $\chi^{(3)}$  charge screening studies indicate that the signal originates from  $5 \times 10^{11}$  strands per square centimeter, or 6 attomoles of surface-bound oligonucleotides. The label-free, molecular-specific nature afforded by nonlinear optical studies of DNA at aqueous/solid interfaces allows for the real-time tracking of interfacial DNA hybridization for the first time.

### Introduction

DNA possesses unique molecular recognition properties that have allowed for the design of exquisitely selective and sensitive biodetection schemes as well as highly functional and specific new materials.<sup>1–5</sup> Unfortunately, although the hybridization of DNA is the key recognition event underlying these technologies and materials, it is much better understood for bulk media<sup>6</sup> than for the heterogeneous environments in which DNA-based devices and materials operate. While important molecular-level information concerning DNA in interfacial environments can be obtained from experiments in which tagged, or labeled, DNA is used,<sup>7–10</sup> label-free probes have the advantage of detecting DNA-based structures at surfaces and interfaces directly and with molecular specificity.<sup>11–15</sup> From a fundamental science perspective and in the context of addressing the demanding

engineering aspects associated with biomedical sensing, experimental strategies in which DNA at interfaces is probed with direct methods that report on the native system are highly desirable. Nonlinear optical spectroscopies<sup>16–19</sup> are beginning to emerge as an important strategy for achieving this objective. Nonlinear optical probes such as second harmonic and sum frequency generation (SHG and SFG) can provide detailed, molecular-level, structural information that is similar to what can be achieved by NMR while at the same time being exquisitely surface selective. Furthermore, the coherent nature of SHG and SFG allow for optical heterodyne signal detection, which is a powerful method for improving the sensitivity of coherent spectroscopies.<sup>20–29</sup>

- (1) Alivisatos, A. P.; Johnsson, K. P.; Peng, X.; Wilson, T. E.; Loweth, C. J.; Bruchez, J.; M. P.; Schultz, P. G. *Nature* **1996**, *382*, 609–611.
- (2) Taton, T. A.; Mirkin, C. A.; Letsinger, R. L. *Science* **2000**, *289*, 1757–1760.
- (3) Seeman, N. C. *Nature* **2003**, *421*, 427–431.
- (4) Kohli, P.; Harrell, C. C.; Cao, Z.; Gasparac, R.; Tan, W.; Martin, C. R. *Science* **2004**, *305*, 984–986.
- (5) Park, S. Y.; Lytton-Jean, A. K. R.; Lee, B.; Weigand, S.; Schatz, G. C.; Mirkin, C. M. *Nature* **2008**, *451*, 553–556.
- (6) Bloomfield, V. A.; Crothers, D. M.; Tinoco, J. I. *Nucleic Acids: Structures, Properties, and Function*; University Science Books: Sausalito, CA, 2000.
- (7) Strother, T.; Cai, W.; Zhao, X.; Hamers, R. J.; Smith, L. M. *J. Am. Chem. Soc.* **2000**, *122*, 1205–1209.
- (8) Finot, E.; Bourillot, E.; Meunier-Prest, R.; Lacroute, Y.; Legay, G.; Cherkaoui-Malki, M.; Latruffe, N.; Siri, O.; Braunstein, P.; Dereux, A. *Ultramicroscopy* **2003**, *97*, 441–449.
- (9) Chrisey, L. A.; U. L. G.; O’Ferrall, C. E. *Nucleic Acids Res.* **1996**, *24*, 3031–3039.
- (10) Jin, R.; Wu, G.; Li, Z.; Mirkin, C. A.; Schatz, G. C. *J. Am. Chem. Soc.* **2003**, *125*, 1643–1654.
- (11) Georgiadis, R.; Peterlinz, K. P.; Peterson, A. W. *J. Am. Chem. Soc.* **2000**, *122* (13), 3166–3173.
- (12) Nelson, B. P.; Grimsrud, T. E.; Liles, M. R.; Goodman, R. M.; M., C. R. *Anal. Chem.* **2001**, *73*, 1–7.
- (13) Wang, J.; Bard, A. J. *Anal. Chem.* **2001**, *73*, 2207–2212.

- (14) Moses, S.; Brewer, S. H.; Lowe, L. B.; Lappi, S. E.; Gilvey, L. B. G.; Sauthier, M.; Tenent, R. C.; Feldheim, D. L.; Franzen, S. *Langmuir* **2004**, *20*, 11134–11140.
- (15) Boncheva, M.; Scheibler, L.; Lincoln, P.; Vogel, H.; Akerman, B. *Langmuir* **1999**, *15*, 4317–4320.
- (16) Boman, F. C.; Musorrafti, M. J.; Gibbs, J. M.; Stepp, B. R.; Salazar, A. M.; Nguyen, S. T.; Geiger, F. M. *J. Am. Chem. Soc.* **2005**, *127*, 15368–15369.
- (17) Stokes, G. Y.; Boman, F. C.; Gibbs-Davis, J. M.; Stepp, B. R.; Condie, A.; Nguyen, S. T.; Geiger, F. M. *J. Am. Chem. Soc.* **2007**, *129*, 7492–7493.
- (18) Wurpel, G. W. H.; Sovago, M.; Bonn, M. *J. Am. Chem. Soc.* **2007**, *129*, 8420–8421.
- (19) Asanuma, H.; Noguchi, H.; Uosaki, K.; Yu, H.-Z. *J. Am. Chem. Soc.* **2008**, *130*, 8016–8022.
- (20) Zanni, M. T.; Gnanakaran, S.; Stenger, J.; Hochstrasser, R. M. *J. Phys. Chem. B* **2001**, *105*, 6520–6535.
- (21) Krummel, A. T.; Mukherjee, P.; Zanni, M. T. *J. Phys. Chem. B* **2003**, *107*, 9165–9169.
- (22) Brixner, T.; Stiopkin, I. V.; Fleming, G. R. *Opt. Lett.* **2004**, *29*, 884–886.
- (23) Demirdoeven, N.; Cheatum, C. M.; Chung, H. S.; Khalil, M.; Knoester, J.; Tokmakoff, A. *J. Am. Chem. Soc.* **2004**, *126*, 7981–7990.
- (24) Xu, Q.-H.; Ma, Y.-Z.; Fleming, G. R. *J. Phys. Chem. A* **2002**, *106*, 10755–10763.
- (25) Lepetit, L. L.; Cheriaux, G.; Joffre, M. *J. Opt. Soc. Am. B* **1995**, *12*, 2467–2474.
- (26) Kaufman, L. J.; Heo, J.; Ziegler, L. D.; Fleming, G. R. *Phys. Rev. Lett.* **2002**, *88*, 207402.

We recently applied SHG and SFG<sup>30,31</sup> as label-free methods to obtain the full thermodynamic state information for single strand DNA at the fused quartz/water interface,<sup>16</sup> and to decipher the molecular structure of surface-tethered oligonucleotides in both single-strand and duplex forms.<sup>32</sup> In this study, we present the first SHG spectra of DNA-functionalized solid/aqueous interfaces, tune the incident laser wavelength to be in two-photon resonance with the electronic  $\pi-\pi^*$  transitions that are intrinsic to the oligonucleotide bases, and take advantage of chiral SHG activity to distinguish between hybridized and dehybridized DNA strands covalently bound to fused quartz/water interfaces. We then use this label-free DNA detection method to track attomoles of surface-bound oligonucleotides as they undergo hybridization with their complementary strands in situ and in real time.

## Experimental Section

Following our previous work,<sup>16,32</sup> we attached thymine oligonucleotides of varying lengths to the flat side of fused quartz hemispheres functionalized with an 11-(trichlorosilyl)undecanoic acid *N*-hydroxysuccinimidyl (NHS) ester. To quantify the number density of the surface-bound DNA strands, SHG  $\chi^{(3)}$  charge screening experiments were carried out on the single strands covalently attached to the fused quartz/water interface by using aliquots of increasing NaCl concentration maintained at constant pH. In the  $\chi^{(3)}$  method,<sup>33</sup> the square root of the measured second harmonic generation (SHG)<sup>30,31</sup> intensity yields the SHG E-field, which can be expressed via a second-order response that contains the second-order nonlinear susceptibility,  $\chi^{(2)}$ , to which one adds a third-order term, according to  $E_{\text{SHG}} = \chi^{(2)} E_{\omega} E_{\omega} + \chi^{(3)} E_{\omega} E_{\omega} \Phi_0$ .<sup>33</sup> This third-order response contains the third-order nonlinear susceptibility,  $\chi^{(3)}$ , the two applied electromagnetic probe fields oscillating at frequency  $\omega$ ,  $E_{\omega}$ , and the interfacial potential,  $\Phi_0$ . The interfacial potential is produced by the interfacial charges, the corresponding spatial distribution of the counter charges, and dipolar arrays of aligned water molecules,<sup>34,35</sup> whose structure<sup>36,37</sup> and dynamics<sup>38</sup> have been studied using vibrational SFG. The localization of the oligonucleotides at the interface and the high sensitivity<sup>16,32,39–41</sup> of the  $\chi^{(3)}$  method to the interfacial potential make the experiment interface specific.

On a molecular level, the interfacial potential aligns the water molecules within the diffuse electrical double layer that is presumably set up at a charged aqueous/solid interface.<sup>42</sup> The third-order response of the aligned water molecules can then contribute to the SHG E-field produced at the interface.<sup>30</sup> If the experiments are carried out at constant pH and varying salt concentration, the measured SHG E-field response yields the interfacial charge density via various electrical double-layer models.<sup>16,33,39–41,43,44</sup> Charge screening experiments were performed on a fused quartz/water interfaces functionalized with oligonucleotides containing 15, 25, 30, and 35 thymine nucleotides. Surface-bound duplexes were formed with T<sub>25</sub>-functionalized substrates that were placed in a 10- $\mu$ M solution of A<sub>25</sub> in pH 7 containing an electrolyte concentration of 0.25 M NaCl.

The sample cell and the detection system have been described previously.<sup>16,45–48</sup> Briefly, we study the flat side of a fused quartz hemisphere (ISP Optics) held leak-tight via a Viton O-ring to a custom-built Teflon cell. The aqueous/solid interface is investigated using the 490–540 nm output (nominally 10 nm bandwidth) produced by mixing the signal and pump light fields from an optical parametric amplifier that is pumped by a kHz regeneratively amplified Ti:Sapphire laser generating 120-fs pulses. A half-waveplate and polarizer cubes are used to select the input and output polarization of the probe and SHG light fields, and the signal detection is carried out using a preamplified single-photon counting system after passing the SHG signal through the appropriate optical filters and a monochromator. At the relevant SHG wavelengths, the reflectivity of the two signal steering mirrors, the transmittivity of the polarization selection optics and the optical filter cutting out the fundamental probe light, the monochromator throughput, and the PMT quantum efficiency result in an estimated 10% conversion of SHG photons generated at the interface to photons counted by the single photon counter. The proper input power dependence of the SHG response from the DNA-functionalized fused quartz/water interface is verified regularly (see Supporting Information). Following our previous SHG spectroscopy work on organic and inorganic adsorbates,<sup>49–54</sup> SHG spectra were recorded by scanning the fundamental wavelength across the two-photon resonance of the interface. Experimental details regarding fluorescence measure-

(27) Vaughan, J. C.; Hornung, T.; Stone, K. W.; Nelson, K. A. *J. Phys. Chem. A* **2007**, *111*, 4873–4883.  
 (28) Stioipkin, I. V.; Jayathilake, H.; Bordenyuk, A. N.; Benderskii, A. V. *J. Am. Chem. Soc.* **2008**, *130*, 2271–2275.  
 (29) Gibbs-Davis, J. M.; Kruk, J. J.; Konek, C. T.; Scheidt, K. A.; Geiger, F. M. *J. Am. Chem. Soc.* **2008**, *130*, 15444–15447.  
 (30) Eisenthal, K. B. *Chem. Rev.* **1996**, *96* (4), 1343–1360.  
 (31) Shen, Y. R. *The Principles of Nonlinear Optics*; John Wiley & Sons: New York, 1984.  
 (32) Stokes, G. Y.; Gibbs-Davis, J. M.; Boman, F. C.; Stepp, B. R.; Condie, A. G.; Nguyen, S. T.; Geiger, F. M. *J. Am. Chem. Soc.* **2007**, *129*, 7492–7493.  
 (33) Zhao, X.; Subrahmanyam, S.; Eisenthal, K. B. *Chem. Phys. Lett.* **1990**, *171*, 558–562.  
 (34) Kendall, T. A.; Martin, S. T. *Geochim. Cosmochim. Acta* **2005**, *69*, 3257–3263.  
 (35) Park, C.; Fenter, P.; Nagu, K. L.; Sturchio, N. C. *Phys. Rev. Lett.* **2006**, *97*, 016101(1–4).  
 (36) Gopalakrishnan, S.; Liu, D.; Allen, H. C.; Kuo, M.; Shultz, M. J. *Chem. Rev.* **2006**, *106* (4), 1155–1175.  
 (37) Scatena, L. F.; Brown, M. G.; Richmond, G. L. *Science* **2001**, *292* (5518), 908–912.  
 (38) McGuire, J. A.; Shen, Y. R. *Science* **2006**, *313*, 1945–1948.  
 (39) Konek, C. T.; Musorrafiti, M. J.; Al-Abadleh, H. A.; Bertin, P. A.; Nguyen, S. T.; Geiger, F. M. *J. Am. Chem. Soc.* **2004**, *126*, 11754–11755.  
 (40) Hayes, P. L.; Malin, J. N.; Konek, C. T.; Geiger, F. M. *J. Phys. Chem. A* **2008**, *112*, 660–668.  
 (41) Malin, J. N.; Hayes, P. L.; Geiger, F. M. *J. Phys. Chem. C* **2008**, *112*, published online November 14, 2008., <http://dx.doi.org/10.1021/jp805068f>.

(42) Adamson, A. W. *Physical Chemistry of Surfaces*, 5th ed.; John Wiley & Sons: New York, 1990.  
 (43) Xiao, X. D.; Vogel, V.; Shen, Y. R. *Chem. Phys. Lett.* **1989**, *163*, 555.  
 (44) Konek, C. T.; Musorrafiti, M. J.; Voges, A. B.; Geiger, F. M. Tracking the Interaction of Transition Metal Ions with Environmental Interfaces Using Second Harmonic Generation. In *Adsorption of Metals by Geomedia II*; Barnett, M., Kent, D., Eds.; Elsevier: New York, 2008; Vol. 7, pp 95–124.  
 (45) Mifflin, A. L.; Gerth, K. A.; Geiger, F. M. *J. Phys. Chem. A* **2003**, *107*, 9620–9627.  
 (46) Al-Abadleh, H. A.; Voges, A. B.; Bertin, P. A.; Nguyen, S. T.; Geiger, F. M. *J. Am. Chem. Soc.* **2004**, *126* (36), 11126–11127.  
 (47) Al-Abadleh, H. A.; Mifflin, A. L.; Bertin, P. A.; Nguyen, S. T.; Geiger, F. M. *J. Phys. Chem. B* **2005**, *109*, 9691–9702.  
 (48) Al-Abadleh, H. A.; Mifflin, A. L.; Musorrafiti, M. J.; Geiger, F. M. *J. Phys. Chem. B* **2005**, *109*, 16852–16859.  
 (49) Mifflin, A. L.; Gerth, K. A.; Weiss, B. M.; Geiger, F. M. *J. Phys. Chem. A* **2003**, *107* (32), 6212–6217.  
 (50) Mifflin, A. L.; Konek, C. T.; Geiger, F. M. *J. Phys. Chem. B* **2006**, *110*, 22577–22585.  
 (51) Mifflin, A. L.; Musorrafiti, M. J.; Konek, C. T.; Geiger, F. M. *J. Phys. Chem. B* **2005**, *109* (51), 24386–24390.  
 (52) Konek, C. T.; Illg, K. D.; Al-Abadleh, H. A.; Voges, A. B.; Yin, G.; Musorrafiti, M. J.; Schmidt, C. M.; Geiger, F. M. *J. Am. Chem. Soc.* **2005**, *127*, 15771–15777.  
 (53) Geiger, F. M.; Tridico, A. C.; Hicks, J. M. *J. Phys. Chem. B* **1999**, *103*, 8205–8215.  
 (54) Geiger, F. M.; Pibel, C. D.; Hicks, J. M. *J. Phys. Chem. A* **2001**, *105*, 4940–4945.

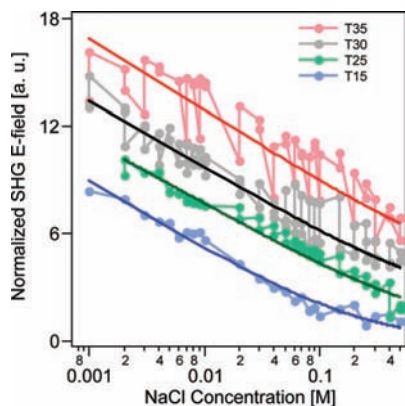


**Figure 1.** p-In/all-out-polarized SHG charge screening of fused quartz substrates functionalized with oligonucleotides containing 15, 25, 30, and 35 thymines (bottom to top). Traces offset for clarity and fit to the Gouy–Chapman–Stern model. Each experiment was carried out in triplicate. Please see text for details.

ments on fluorescein-tagged DNA oligonucleotides are described in the Supporting Information.

## Results and Discussion

To quantify the number density of the surface-bound DNA strands, we screened the interfacial charges along the DNA backbone by adding increasing amounts of NaCl to the aqueous solution above the surface while recording the SHG signal intensity. Each charge screening experiment was carried out in triplicate, the data were normalized to the SHG intensity at the highest salt concentration, and the results are shown in Figure 1 for oligonucleotides containing 15, 25, 30, and 35 thymine nucleotides.

As expected from our earlier work on DNA oligonucleotide-functionalized surfaces,<sup>16</sup> the SHG E-field decreases with increasing salt concentration, which is attributed to charge screening of the phosphate backbone by the electrolyte. Given the versatility of the Gouy–Chapman–Stern model<sup>55</sup> in describing the surface behavior of a variety of analytes over a wide range of ionic strengths,<sup>56–64</sup> we apply it to our data. As discussed in recently published work,<sup>41,65</sup> the Gouy–Chapman model fails at high surface charge densities and interfacial potentials exceeding  $\sim 100$  mV at which point the potential sensitivity on surface charge density, and thus the SHG sensitivity, becomes highly nonlinear. Such problems are not encountered with the Gouy–Chapman–Stern model because

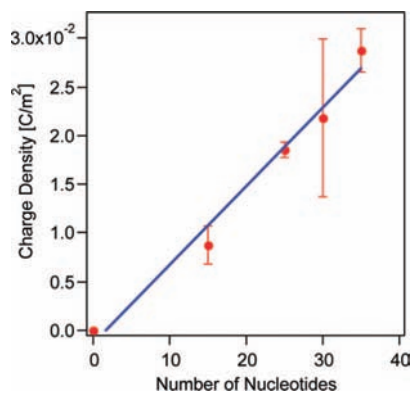


**Figure 2.** Interfacial charge density obtained from fitting Gouy–Chapman–Stern theory to the charge screening data shown in Figure 1 as a function of oligonucleotide length. The straight line is a linear least-squares fit to the data.

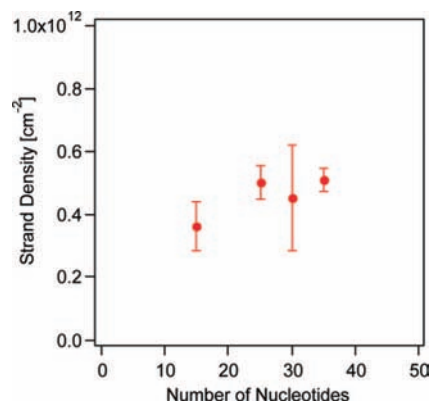


**Figure 3.** Interfacial DNA oligonucleotide strand density as a function of oligonucleotide length.

the metal ions are placed in the Stern layer and the changes in charge density due to metal ion adsorption are treated using a constant capacitance approach. In this case, the potential continues to increase in a roughly linear fashion with ion concentration no matter how much interfacial charge is accumulated, leading to lower and more reasonable charge densities obtained from the fits.

The interfacial charge densities obtained from the Gouy–Chapman–Stern model fit to our data increase linearly with the number of nucleotides (Figure 2). The slope of a linear least-squares fit results in 1.0(1) charges per added nucleotide, which is consistent with the notion that each nucleotide carries a charge of  $-1$  on the phosphate group.

Taking the interfacial charge density and dividing it by the elemental charge and the number of nucleotides in the DNA strand yields a DNA oligonucleotide strand density of around  $5 \times 10^{11}$  per cm<sup>2</sup> (Figure 3). Given that we are studying the aqueous/solid interface with a focused laser beam illuminating a 30- $\mu$ m diameter spot, we conclude that the SHG response comes from only 6 attomoles of DNA at the interface. This remarkable sensitivity can be attributed to the self-heterodyning nature of the experiment, in which the second-order response can be viewed as the local oscillator, while the third-order terms can be considered the signal.<sup>29</sup> We note that the experiments presented here probe the states of native, label-free DNA oligonucleotides.

After quantifying the amount of DNA oligonucleotides in the laser spot using the  $\chi^{(3)}$  method, we characterized them at the

- (55) Stumm, W.; Morgan, J. J. *Aquatic Chemistry*, 3rd ed.; Wiley-Interscience: New York, 1996.
- (56) Brown, G. E.; Henrich, V. E.; Casey, W. H.; Clark, D. L.; Eggleston, C.; Felmy, A.; Goodman, D. W.; Gratzel, M.; Maciel, G.; McCarthy, M. I.; Nealon, K. H.; Sverjensky, D. A.; Toney, M. F.; Zachara, J. M. *Chem. Rev.* **1999**, *99*, 77–174.
- (57) Hayes, K. F.; Redden, G.; Ela, W.; Leckie, J. O. *J. Colloid Interface Sci.* **1991**, *142* (2), 448–469.
- (58) Koopal, L. K. *Electrochim. Acta* **1996**, *41* (14), 2293–2305.
- (59) Kosmulski, M. *Colloids Surf., A* **1996**, *117* (3), 201–214.
- (60) Langmuir, D. *Aqueous Environmental Geochemistry*; Prentice Hall: Upper Saddle River, NJ, 1997.
- (61) Morel, F. M. M.; Hering, J. G. *Principles and Applications of Aquatic Chemistry*; John Wiley & Sons, Inc.: New York, 1993.
- (62) Robertson, A. P.; Leckie, J. O. *J. Colloid Interface Sci.* **1997**, *188* (2), 444–472.
- (63) Sahai, N.; Sverjensky, D. A. *Geochim. Cosmochim. Acta* **1997**, *61* (14), 2801–2826.
- (64) Yates, D. E.; Levine, S.; Healy, T. W. *J. Chem. Soc., Faraday Trans. I* **1974**, *70*, 1807–1818.
- (65) Geiger, F. M. *Annu. Rev. Phys. Chem.* **2009**, *60*, 61–83.

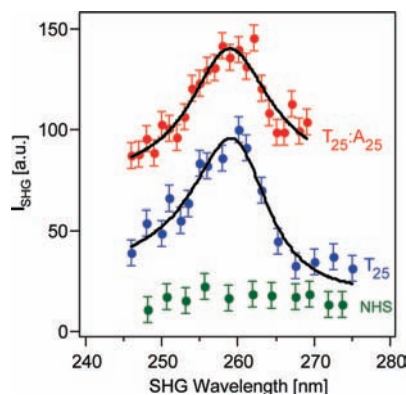


**Figure 4.** p-In/all-out-polarized SHG spectra of fused quartz/water interfaces functionalized with the NHS linker (bottom, filled green circles),  $T_{25}$  oligonucleotides (middle, filled blue circles), and the surface-bound (sb)- $T_{25}:A_{25}$  duplex (top, filled red circles). Black lines are Lorentzian fits to the data. Each spectrum represents the average of at least three independent measurements. Spectra are offset for clarity.

solid/aqueous interface using resonantly enhanced SHG. This spectroscopic characterization would, in principle, allow us to carry out linear dichroism experiments for tracking DNA hybridization directly at an interface. This can be understood as follows: if a double helix (A or B) were to form between the 3'-surface-bound DNA and its complementary strand, it should be right-handed, antiparallel,<sup>6</sup> and exhibit a nonlinear optical chiral response that is different from that of the single strands, which do not form a helix under our experimental conditions. Given previous work on resonantly enhanced SHG studies of chiral systems,<sup>66–71</sup> this difference in the nonlinear optical chiral response of surface-bound DNA oligonucleotides should be particularly pronounced when the experiment is conducted on electronic resonance.

To determine the wavelengths at which maximal two-photon resonance occurs in our system, we first recorded the SHG spectra of the NHS linker-functionalized fused quartz/water interface, the  $T_{25}$  single strand-functionalized fused quartz/water interface, and the  $T_{25}$  single strand-functionalized fused quartz/water interface duplexed with the complementary  $A_{25}$  strand. The results are shown in Figure 4. All spectra were recorded *in situ* at the aqueous/solid interface, at pH 7, in the presence of 0.25 M NaCl, and in triplicate. The energy of the fundamental probe light field was maintained at  $0.75 \mu\text{J}$ , which is well below the damage threshold (see Supporting Information). A Lorentzian fit to the SHG spectra<sup>72</sup> shows that the electronic resonance occurs at  $258.1(1) \text{ nm}$  with a  $6(1) \text{ nm}$  half-width-at-half-maximum for the  $T_{25}$  single strand, and at  $260(1) \text{ nm}$  with a  $6(1) \text{ nm}$  half-width-at-half-maximum for the  $T_{25}:A_{25}$  duplex. These results are consistent with the strong  $\pi-\pi^*$  transitions

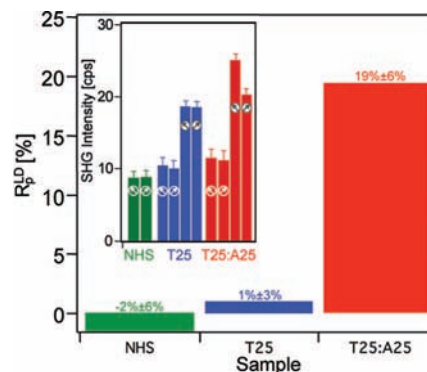


**Figure 5.** p-Polarized SHG-LD response at 260 nm of fused quartz/water interfaces functionalized with NHS (left, green bar),  $T_{25}$  oligonucleotides (center, blue bar), and the sb- $T_{25}:A_{25}$  duplex (right, red bar). (Inset)  $\pm 45^\circ$  p-polarized SHG responses off and on two-photon resonance (250 nm, empty circles, and 260 nm, filled circles, respectively) for the same samples. +45 = left-pointing arrows, -45 = right-pointing arrows. Data entries are averaged over at least three independent measurements, samples, and laser spot positions.

of thymine and adenine bases that are present in the single strand and the duplex.<sup>73,74</sup>

To determine the p-polarized SHG linear dichroic (SHG-LD) ratios for the  $T_{25}$  single strand and the  $T_{25}:A_{25}$  duplex, we recorded the p-polarized SHG intensity obtained when probing the interface with light fields plane-polarized at  $+45^\circ$  and  $-45^\circ$  from the surface normal. This signal detection scheme is akin to self-heterodyne detection of the weak SHG E-field obtained with the chirality-selective p-in/s-out polarization combination while using the strong E-field generated using the p-in/p-out polarization combination, which probes achiral signal contributions, as the local oscillator.<sup>32</sup> When divided by their average, the difference in the two SHG intensities obtained for each experiment yields the SHG-LD ratio.<sup>66,68,69</sup>

The results from these experiments are shown in Figure 5. As expected, the SHG-LD ratio of the achiral NHS linker is negligible. For the nucleotides, we determined the SHG-LD ratios at wavelengths on and off electronic resonance. When we tune the incident wavelength to be in two-photon resonance with the  $\pi-\pi^*$  transitions of the bases (i.e., at an SHG wavelength of 260 nm), the  $T_{25}$  single strand exhibits only a slight SHG-LD response that falls within the uncertainty of the measurement. In contrast, the surface-bound (sb)- $T_{25}:A_{25}$  duplex exhibits a strong SHG-LD response ( $19 \pm 6\%$ ) on resonance but again no SHG-LD response when the incident wavelength is tuned away from two-photon resonance. Each hybridization experiment was carried out without changing the optical alignment, the sample cell location, and the laser spot position. The inset in Figure 5 shows the average number of SHG photons counted per second for the experiments presented here. Interestingly, when the incident wavelength is tuned either away from or onto two-photon resonance, the  $\pm 45^\circ$  in/p-out polarization combination yields, on average and within error, as many SHG counts for the  $T_{25}:A_{25}$  duplex as for the  $T_{25}$  single strand. The substantial increase in the SHG-LD response when going from the  $T_{25}$  single strand to the sb- $T_{25}:A_{25}$  duplex is thus mainly due to the signal yield obtained from the  $\pm 45^\circ$  in/p-out polarization combination. We note that it would be challenging to

(66) Petralli-Mallow, T.; Maeda-Wong, T.; Byers, J. D.; Yee, H. I.; Hicks, J. M. *J. Phys. Chem.* **1993**, *97* (7), 1383–1388.

(67) Simpson, G. J. *ChemPhysChem.* **2004**, *5*, 1301–1310.

(68) Maki, J. J.; Verbiest, T.; Kauranen, M.; Van Elshocht, S.; Persoons, A. *J. Chem. Phys.* **1996**, *105*, 767.

(69) Plocinik, R. M.; Everly, M.; Moad, A. K.; Simpson, G. J. *Phys. Rev. B: Condens. Mater. Sci.* **2005**, *72*, 125409–125422.

(70) Verbiest, T.; Van Elshocht, S.; Persoons, A.; Nuckols, C.; Phillips, K. E.; Katz, T. J. *Langmuir* **2001**, *17*, 4685–4687.

(71) Wampler, R. D.; Kissick, D. J.; Dehen, C. J.; Gualtieri, E. J.; Grey, J. L.; Wang, H.-F.; Thompson, D. H.; Cheng, J.-X.; Simpson, G. J. *J. Am. Chem. Soc.* **2008**, *130*, 14076–14077.

(72) Steel, W. H.; Walker, R. A. *Nature* **2003**, *424*, 296.

(73) Lorentzon, J.; Fuelscher, M. P.; Roos, B. O. *J. Am. Chem. Soc.* **1995**, *117*, 9265–9273.

(74) Fuelscher, M. P.; Serrano-Andres, L.; Roos, B. O. *J. Am. Chem. Soc.* **1997**, *119*, 6168–6176.

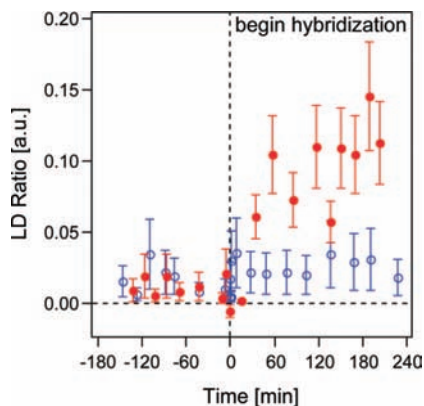


**Figure 6.** Real time SHG-LD response recorded on resonance at 260 nm (filled circles) and off resonance at 250 nm (empty circles) from fused quartz surfaces functionalized with T<sub>25</sub> ssDNA during hybridization with A<sub>25</sub> ssDNA strands in a 0.2 M NaCl solution started at  $t = 0$  as indicated by the vertical dashed line.

observe these chiral responses from subfemtomole amounts of DNA with other label-free detection methods.

Our experimental results prompted us to track the SHG-LD response of DNA oligonucleotides at 260 nm (i.e., on electronic resonance, as a function of time during hybridization). The results are shown in Figure 6, which reveals that the hybridization process causes an increase in the SHG-LD, consistent with the data shown in Figure 5. As expected from the data displayed in Figure 5, the SHG LD ratio does not change beyond what is observed for the single strand when the laser is tuned off electronic resonance. Complementary fluorescence measurements, carried out in similar time steps but with an off-line

approach utilizing many samples whose hybridization process was stopped at a given time  $t$  for the off-line measurement, show a similar response (see Supporting Information).

### Summary

In conclusion, we have successfully obtained electronic spectra of single-strand and duplex DNA oligonucleotides covalently attached to fused quartz/aqueous interfaces. We have demonstrated that a strong nonlinear optical linear dichroism response is obtained when adenine and thymine bases undergo Watson–Crick base pairing to form a double helix. These are the first measurements of electronic signatures from surface-bound DNA and their chirality. Given the label-free, molecularly specific nature afforded by nonlinear optical studies of DNA at aqueous/solid interfaces, real-time investigations of interfacial DNA hybridization and melting are now possible on the native system, as demonstrated in Figure 6. The results obtained from these experiments should lead to improved biondiagnostic applications and new biologically relevant materials.

**Acknowledgment.** This work was supported by the Northwestern University Nanoscale Science and Engineering Center (NSEC), an NSF Experimental Physical Chemistry CAREER Grant No. CHE-0348873 (F.M.G.), the Camille and Henry Dreyfus Foundation Environmental Chemistry Postdoctoral Program (J.G.D.), and the Sloan foundation (F.M.G.).

**Supporting Information Available:** Details regarding the complementary fluorescence measurements, control studies, and synthetic procedures. This material is available free of charge via the Internet at <http://pubs.acs.org>.

JA808007B